Effect of Propylene Glycol Coolant pH on the Galvanic Corrosion Behavior of 6061 Aluminum Alloy/304 Stainless Steel

Hao Miao , Cong Shao , Jinqiao Zheng , Hao Yu , Heqian Wang , Kui Xiao *

Posted Date: 3 June 2026

doi: 10.20944/preprints202606.0260.v1

Keywords: propylene glycol coolant; aluminum alloy; stainless steel; galvanic corrosion; pH value

 doi:10.20944/preprints202606.0260.v1

Article

Effect of Propylene Glycol Coolant pH on the Galvanic Corrosion Behavior of 6061 Aluminum Alloy/304 Stainless Steel

Hao Miao [1], Cong Shao [2], Jinqiao Zheng [2], Hao Yu [1], Heqian Wang [1] and Kui Xiao [1,*]

[1] Institute for Advanced Materials and Technology, University of Science and Technology Beijing, Beijing 100083, China

[2] ZTE Corporation, Shenzhen 518057, China

* Correspondence: xiaokui@ustb.edu.cn

Abstract

6061 aluminum alloy is lightweight and has good thermal conductivity, while 304 stainless steel possesses excellent mechanical properties and corrosion resistance; both have broad application prospects in cooling circuits. Propylene glycol coolant shows great potential in liquid cooling systems due to its low toxicity and good antifreeze properties. However, during operation, galvanic corrosion may occur when the two metals come into direct contact within the coolant, thereby threatening system safety and service life. This study focuses on 6061 aluminum alloy, 304 stainless steel, and their galvanic couples. Using electrochemical testing, SEM, 3D confocal microscopy, and XPS to systematically investigate their self-corrosion and galvanic corrosion behavior in propylene glycol coolant at pH values of 4.8, 6.8, and 8.8. The results indicate that 6061 aluminum alloy is more sensitive to pH changes; its corrosion resistance first increases and then decreases as pH rises, with the least corrosion occurring at pH = 6.8 and the most severe at pH = 4.8. 304 stainless steel exhibited lower corrosion rates at pH 6.8 and 8.8, but corrosion significantly worsened at pH 4.8. For the 6061 aluminum alloy/304 stainless steel couple, the galvanic current first decreased and then increased with rising pH, while the galvanic potential first increased and then decreased. The 6061 aluminum alloy consistently acted as the anode, and the 304 stainless steel consistently acted as the cathode, with the highest sensitivity to galvanic corrosion observed at pH 4.8. XPS analysis shows that under different pH conditions, the corrosion products of 6061 aluminum alloy are $Al(OH)_3$ and Al_2O_3, while the main components of the passivation film on 304 stainless steel remain unchanged.

Keywords: propylene glycol coolant; aluminum alloy; stainless steel; galvanic corrosion; pH value

1. Introduction

With the continuous advancement of liquid cooling technology in the automotive, aerospace, new energy, and data center sectors, coolants are playing an increasingly critical role in ensuring system safety and efficient heat transfer. To meet the demands of high power density and high reliability, coolants must possess excellent heat transfer properties, freeze resistance, thermal stability, material compatibility, and long-term operational stability [1–3]. In actual liquid cooling systems, components such as cold plates, piping, fittings, valve bodies, manifolds, and heat exchangers are often composed of different metallic materials. Among these, aluminum alloys are lightweight and have excellent thermal conductivity, making them commonly used for cold plates, heat dissipation structures, and heat exchange components; stainless steel, with its high mechanical strength and corrosion resistance, is frequently used for piping, fittings, valve bodies, and connecting structures [4]. Aluminum alloys and stainless steel are frequently used in combination within cooling circuits; however, direct contact between the two may trigger galvanic corrosion [5]. Consequently, aluminum alloys and stainless steel are often paired in cooling systems based on the specific functions

 doi:10.20944/preprints202606.0260.v1

of different components, and their material compatibility significantly influences the stable operation of the cooling system.

Currently, the mainstream coolants in engineering applications are ethylene glycol/water and propylene glycol/water systems, both of which can adjust freezing and boiling points to meet the requirements of operation across a wide temperature range [6]. Ethylene glycol-based coolants have low viscosity and high heat transfer efficiency, but they are prone to oxidation at high temperatures, producing acidic byproducts such as glycolic acid and oxalic acid, which cause a drop in pH. This can damage the passivation films on the surfaces of aluminum alloys and stainless steel, inducing failure modes such as pitting corrosion and crevice corrosion [7]. Although pure ethylene glycol can inhibit the anodic dissolution of aluminum alloys and form protective aluminum-alcohol products, its oxidation products still significantly exacerbate corrosion under long-term high-temperature service conditions [8–10]. For stainless steel, the acidic medium generated by the oxidation of ethylene glycol weakens the density of the passivation film, increasing the risk of pitting corrosion [11–13]. In contrast, propylene glycol-based coolants are less toxic and offer better environmental compatibility and operational safety [14,15], demonstrating greater application potential in scenarios such as data center cold plates [16,17] and new energy vehicle cooling systems [18]. Studies indicate that propylene glycol has a corrosion-inhibiting effect on aluminum alloys; the mechanism involves alcohol molecules adsorbing onto the metal surface to form an aluminum–alcohol passivation film, thereby slowing corrosion of the aluminum alloy [19,20]. However, aluminum alloys remain highly sensitive to temperature, Cl^-, and pH in propylene glycol environments, making them prone to pitting and localized accelerated corrosion [21]. Stainless steel is generally more stable in similar environments, but when aluminum comes into direct contact with stainless steel and is used in conjunction with conductive organic coolants, there is a risk of galvanic corrosion [22,23].

During long-term operation of liquid-cooling systems, the oxidation and degradation of the cooling medium or the dissolution of ambient gases can cause changes in the pH of the coolant, which in turn affects the stability of the passivation or oxidation layers on metal surfaces and alters the corrosion susceptibility of the materials [24]. Generally speaking, under acidic conditions, surface films are prone to dissolution, leading to accelerated corrosion; under near-neutral conditions, the films are relatively stable; and under alkaline conditions, OH^- ions may cause localized damage to the films, resulting in a renewed increase in corrosion susceptibility [25,26]. A study on the corrosion behavior of 7A09 aluminum alloy in propylene glycol coolant under different pH conditions found that at pH = 4, the surface oxide film of the aluminum alloy underwent acid dissolution, resulting in the most severe corrosion; under near-neutral conditions, propylene glycol interacted synergistically with the oxide film to form a stable protective film, significantly reducing the corrosion rate; at pH = 9, OH^- caused localized dissolution of the passivation film, leading to a renewed increase in corrosion severity [27]. Research has shown that in ethylene glycol–water solutions, higher pH values enhance the corrosive effect of glycolic acid on AA6061 aluminum alloy. The mechanism involves the formation of complexes between glycolic acid and aluminum ions, which promotes the dissolution of the aluminum matrix [28]. In actual liquid cooling systems, when aluminum alloys come into direct contact with dissimilar metals such as stainless steel, an electrochemical couple is formed in the electrolyte environment of the coolant due to the potential difference between the two, leading to accelerated corrosion of the more active metal (aluminum alloy) [29–32]. A study on the effect of pH on the galvanic corrosion behavior of a three-metal couple consisting of 2024 aluminum alloy, Q235 carbon steel, and 304 stainless steel showed that pH significantly alters the anodic dissolution behavior of the aluminum alloy in the galvanic system [33]. In mixed-metal cooling systems, cations generated by the corrosion of copper or iron alloys deposit on the surface of less active alloys (such as aluminum), forming localized cathodes and significantly increasing the risk of localized corrosion [34].

Therefore, this paper focuses on 6061 aluminum alloy and 304 stainless steel—materials commonly used in liquid cooling systems for data centers. While aluminum alloys offer excellent thermal conductivity, they are relatively sensitive to acidic and alkaline environments. During actual

 doi:10.20944/preprints202606.0260.v1

service, when paired with stainless steel—which possesses a chromium-rich passivation film and excellent corrosion resistance—galvanic corrosion is likely to occur. Using a 25% propylene glycol coolant, this study investigates the corrosion behavior of 6061 aluminum alloy, 304 stainless steel, and their galvanic couples under different pH conditions, providing a theoretical basis for optimizing the pH range of coolants and enhancing corrosion protection in liquid cooling systems.

2. Materials and Methods

2.1. Experimental Materials and Coolant

The chemical composition (wt/%) of the 6061 aluminum alloy (T6 condition) used in this study is as follows: 1.08 Mg, 0.68 Si, 0.51 Fe, 0.31 Cu, 0.16 Mn, 0.02 Zn, 0.29 Cr; The chemical composition (wt/%) of 304 stainless steel is: 18.25% Cr, 8.18% Ni, 0.06% C, 1.04% Mn, 0.56% Si, 0.02% S, 0.03% P, and 0.07% Cu. The specimens were machined using wire cutting into two sizes: 10×10×2 mm and 50×25×2 mm, for use in electrochemical testing and corrosion immersion testing, respectively. For the corrosion immersion specimens, a small hole with a diameter of 3 mm was drilled 5 mm from the top of the specimen to facilitate suspension. After machining, the specimens were sanded to a polished finish, rinsed with deionized water, immersed in anhydrous ethanol for 5 minutes, wiped clean with lint-free cotton, and wrapped in non-woven fabric after drying for later use.

The base coolant used in the experiments consists of 75% deionized water and 25% propylene glycol (analytical grade, ≥99.5%) by volume. The pH of the acidic coolant is adjusted using hydrochloric acid, while the pH of the alkaline coolant is adjusted using sodium hydroxide.

2.2. Coolant Corrosion Test Method

Refer to the standard GB 29743.2-2025 regarding the total area of metal specimens and the required volume of cooling fluid; specifically, 7 metal specimens measuring 50 × 25 mm require 750 mL of cooling fluid. In accordance with the aforementioned standard, add the corresponding volume of coolant to the beaker based on the number of metal specimens inside. When studying the self-corrosion behavior of metals in coolant, suspend the specimens in a 1000 mL beaker with the liquid level 20 mm below the top of the container; when studying galvanic corrosion of metals in coolant, maintain a spacing of 25 mm between the galvanic couple and the specimen diameters, and use wires to encapsulate the metal specimens to establish electrical contact. Additionally, to simulate the actual operating temperature of the coolant in data center liquid cooling systems, a constant-temperature chamber was used during the experiment to maintain a temperature of 80 °C.

2.3. Corrosion Testing and Analysis Methods

2.3.1. Corrosion-induced weight loss

Since stainless steel exhibits good corrosion resistance in coolant, this study focuses on the removal of corrosion products from aluminum alloys and the analysis of corrosion weight loss. In accordance with GB/T 16545-2015, pure nitric acid was used to remove corrosion products from the specimen surfaces, which were then weighed (to the nearest 0.01 mg). The corrosion rate (g/m^2) was calculated based on the weight loss.

2.3.2. Characterization of Corrosion Products

A FEI Quanta 250 scanning electron microscope (SEM) was used to observe the microscopic corrosion morphology on the sample surface; a KEYENCE VK200 confocal microscope was used to examine the morphology of pitting corrosion pits on the samples after rust removal; A Thermo Fisher Sigma Probe X-ray photoelectron spectrometer (XPS) was used to analyze the chemical states of elements in the surface products of the samples. The test voltage was set to 15 kV, and measurements

 doi:10.20944/preprints202606.0260.v1

were performed using monochromatic Al Kα X-rays with a step size of 0.05 eV. The data were then analyzed using Advantage software.

2.3.3. Electrochemical Testing

AC impedance and polarization curve tests were performed using a CS 350H electrochemical workstation with a three-electrode system: working electrodes—6061 aluminum alloy (1 cm^2) and 304 stainless steel (1 cm^2); reference electrode—saturated calomel electrode (SCE); and counter electrode—platinum foil (1 × 1 cm). The open-circuit potential (OCP) was stabilized for 30 minutes. AC impedance spectroscopy was performed at frequencies ranging from 100 kHz to 10 mHz. Polarization scans were conducted at ±500 mV vs. OCP (6061 aluminum alloy) and -500 mV to 2000 mV vs. OCP (304 stainless steel), with a scan rate of 0.5 mV/s. The test solutions used for electrochemical testing were propylene glycol coolants under various environmental conditions.

2.3.4. Galvanic Corrosion Testing and Analysis

A CST 508 multi-channel galvanic corrosion tester was used to measure the galvanic current and potential between 6061 aluminum alloy and 304 stainless steel. The active area of each specimen was 1 cm^2, and the distance between the 6061 aluminum alloy and the 304 stainless steel was 25 mm. The 6061 aluminum alloy was connected to WE1, the 304 stainless steel to WE2, and SCE to RE. The total test duration was 20 hours, comprising 4 hours of high-frequency testing, 8 hours of medium-frequency testing, and 8 hours of low-frequency testing.

The average galvanic current is calculated using the integration method based on the galvanic current-time curve, and the average galvanic current density is then determined based on the actual area of the anode in the galvanic cell. The calculation formula is as follows:

$$i_g = \frac{\int_0^t I_g(t)dt}{S \times t} \quad (1)$$

In the equation, $I_g(t)$ represents the galvanic current at time t (A); S represents the effective working area of the anode specimen (cm^2); and t represents the test duration (h).

In accordance with HB5374–1987, the galvanic corrosion susceptibility of 6061 aluminum alloy/304 stainless steel galvanic couples in propylene glycol coolants with three different pH values was classified.

Table 1. Criteria for evaluating galvanic corrosion susceptibility.

Electrode couple current density μA/cm^2	Electrochemical couple corrosion sensitivity rating
$i_g \leq 0.3$	A
$0.3 < i_g \leq 1.0$	B
$1.0 < i_g \leq 3.0$	C
$3.0 < i_g \leq 10.0$	D
$i_g \geq 10.0$	E

3. Results

3.1. Corrosion-induced weight loss

After immersing 6061 aluminum alloy (single metal) and a 6061/304 galvanic couple in propylene glycol coolant at different pH levels for 14 days, rust was removed from the 6061 aluminum alloy and the weight was measured. The corrosion rates under different test conditions were calculated, as shown in Figure 1. As shown in Figure 1, corrosion weight loss for both the single metal and the galvanic couple was highest at pH = 4.8, lowest at pH = 6.8, and intermediate at pH = 8.8. This indicates that a near-neutral environment is conducive to maintaining the stability of the

 doi:10.20944/preprints202606.0260.v1

aluminum alloy's surface oxide film, while both acidic and weakly alkaline conditions promote corrosion. Under pH 4.8 conditions, the acidic environment accelerated the dissolution of the aluminum alloy's surface protective film, making the substrate more susceptible to exposure, resulting in the greatest corrosion weight loss; at pH 6.8, the surface film was relatively stable, corrosion was inhibited, and weight loss was minimal; whereas under pH 8.8 conditions, aluminum and its oxides/hydroxides may undergo amphoteric dissolution, weakening the protective function of the film layer and causing a slight increase in corrosion weight loss. Compared to the single-metal state, the corrosion weight loss of 6061 aluminum alloy after galvanic coupling increased significantly under all three pH conditions, indicating accelerated dissolution when coupled with 304 stainless steel as the anode; the galvanic effect promoted the corrosion process of the 6061 aluminum alloy.

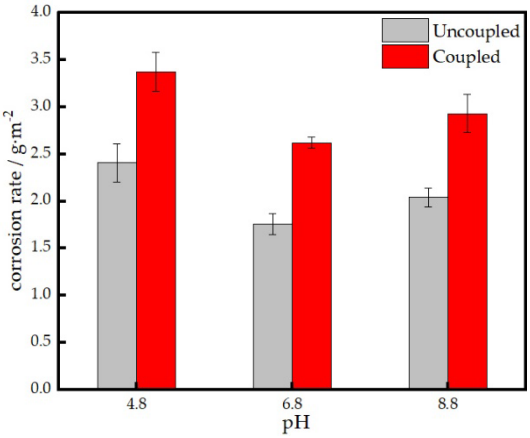

Figure 1. Corrosion rates of 6061 aluminum alloy after immersion in propylene glycol coolant with different pH values for 14 days: uncoupled condition and galvanically coupled with 304 stainless steel.

3.2. Corrosion Morphology and Product Analysis

Figure 2 shows the microstructural corrosion morphology of the anode material (6061 aluminum alloy) in a galvanic couple and the 6061 aluminum alloy in a single-metal state after 14 days of immersion in propylene glycol coolant at different pH levels. As shown in Figure 2, the surface morphology of the 6061 aluminum alloy in the single-metal state changes significantly with pH. At pH = 4.8, the specimen surface exhibited significant accumulation of corrosion products and localized corrosion pits, indicating that the acidic environment promoted the dissolution and destruction of the aluminum alloy's surface oxide film. At pH = 6.8, the specimen surface was relatively smooth with few corrosion products, showing only a small number of scattered corrosion defects. This suggests that the surface film of 6061 aluminum alloy in near-neutral propylene glycol coolant is relatively stable and exhibits good corrosion resistance. When the pH rose to 8.8, localized corrosion products and areas of film damage reappeared on the surface, which is related to the amphoteric dissolution of aluminum and its oxides/hydroxides in a weakly alkaline environment. Compared to the single-metal state, the surface corrosion characteristics of 6061 aluminum alloy were more pronounced after galvanic coupling. Under pH = 4.8 conditions, the surface of the coupled specimens exhibited denser corrosion pits and uneven corrosion products, indicating that galvanic action in an acidic environment further accelerated the anodic dissolution of the 6061 aluminum alloy. Under pH = 6.8 conditions, the surface of the coupled specimens remained relatively smooth with relatively mild corrosion, suggesting that a near-neutral environment can mitigate galvanic corrosion to some extent. Under pH = 8.8 conditions, the surface of the coupled specimens exhibited obvious localized corrosion product coverage, as well as cracking or peeling of the protective film. This indicates that the stability of the aluminum alloy surface film decreases in a weakly alkaline environment, and the galvanic coupling effect further promotes the development of localized corrosion.

 doi:10.20944/preprints202606.0260.v1

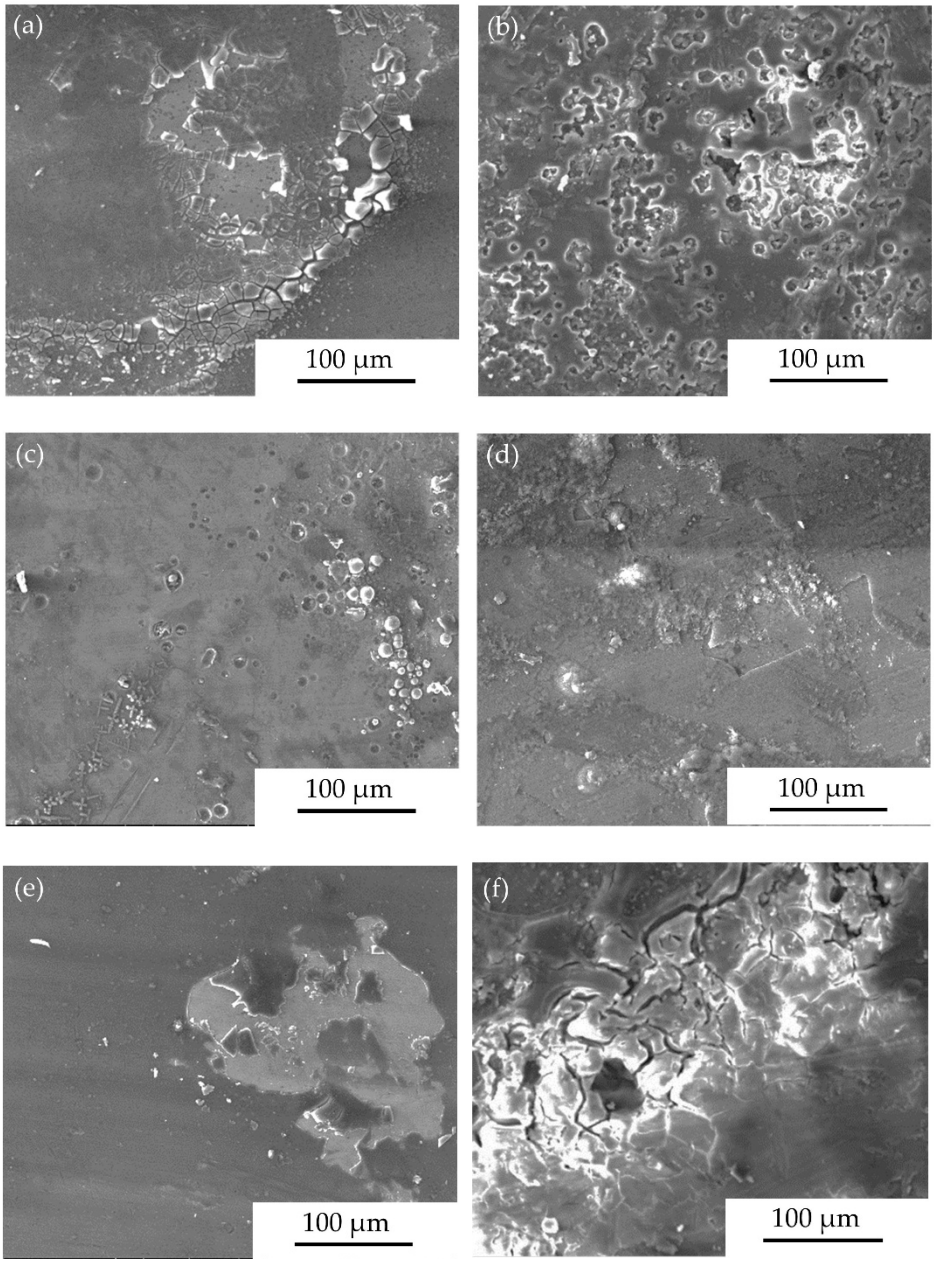

Figure 2. SEM surface morphologies of 6061 aluminum alloy after immersion in propylene glycol coolant with different pH values for 14 days: (a,c,e) uncoupled condition at pH 4.8, 6.8 and 8.8, respectively; (b,d,f) galvanically coupled with 304 stainless steel at pH 4.8, 6.8 and 8.8, respectively.

Figure 3 shows the 3D confocal morphologies of the 6061 aluminum alloy anode material in a galvanic couple and the single-metal 6061 aluminum alloy after rust removal in propylene glycol coolant at different pH levels. When the propylene glycol solution has a pH of 4.8, the corrosion pit depth of the coupled 6061 aluminum alloy reaches approximately 22 μm, with a width of about 172 μm, indicating more severe corrosion compared to the uncoated 6061 aluminum alloy; in propylene glycol coolant with a pH of 6.8, no significant corrosion pits were observed on the surfaces of either the coupled or uncoated 6061 aluminum alloys; When the pH of the propylene glycol coolant was 8.8, extensive spalling occurred in localized areas on the surface of the 6061 aluminum alloy in both states. This indicates that under slightly alkaline conditions, although aluminum alloys typically possess a certain degree of passivation capability, excessively high pH may cause localized destabilization or dissolution of the surface film, leading to a resurgence of localized corrosion.

 doi:10.20944/preprints202606.0260.v1

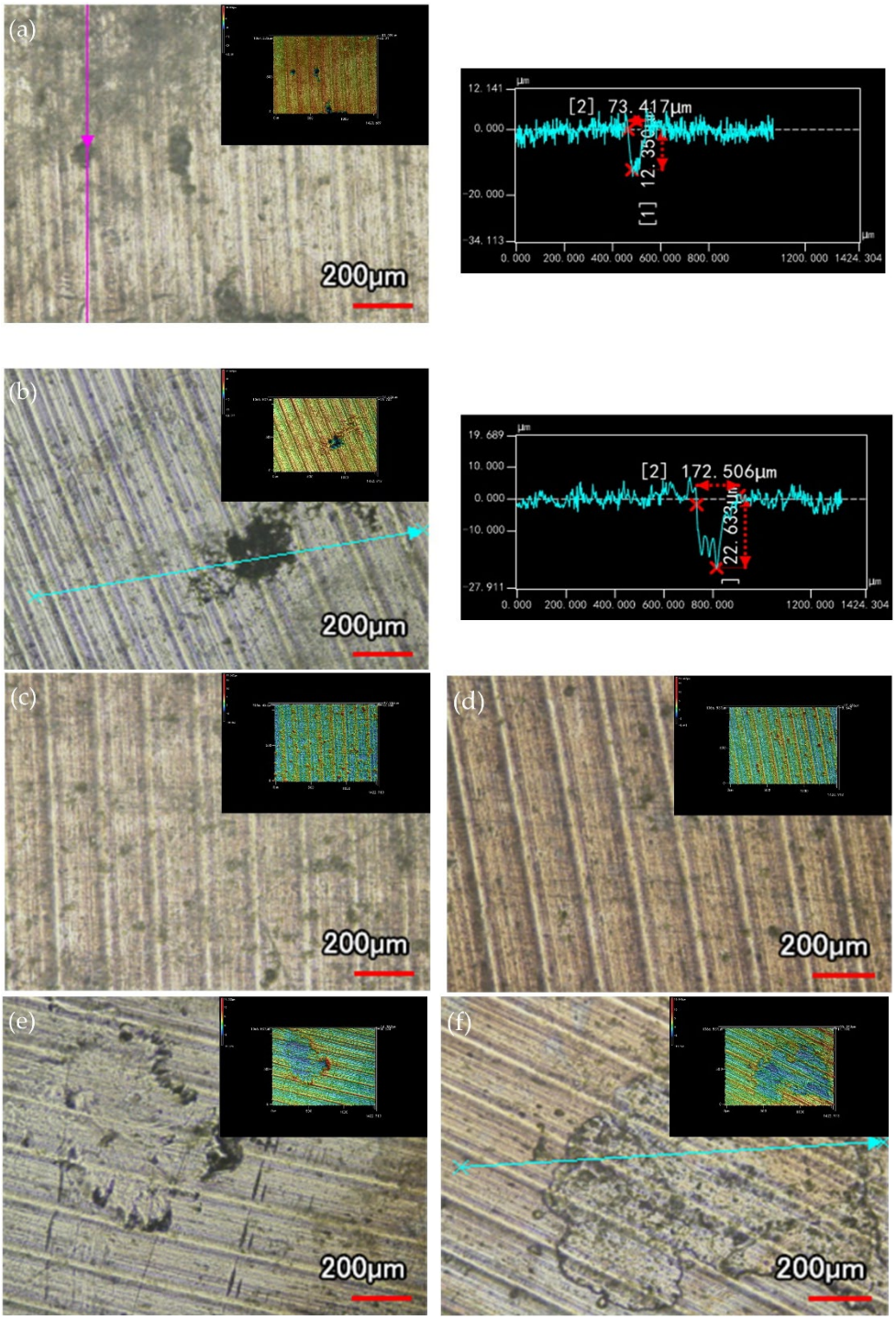

Figure 3. 3D laser confocal morphologies of 6061 aluminum alloy after immersion in propylene glycol coolant with different pH values for 14 days and removal of corrosion products: (a,c,e) uncoupled condition at pH 4.8, 6.8 and 8.8, respectively; (b,d,f) galvanically coupled with 304 stainless steel at pH 4.8, 6.8 and 8.8, respectively.

Figures 4–6 show the XPS spectra and the composition of various substances for 6061 aluminum alloy and 304 stainless steel after 14 days of immersion in propylene glycol coolant at different pH levels. As shown in Figure 4, the main components of the corrosion products of 6061 aluminum alloy in propylene glycol coolant at different pH levels remained unchanged, consisting primarily of $Al(OH)_3$ and Al_2O_3. Under different pH conditions, the C 1s spectrum of the 6061 aluminum alloy exhibited three peaks, corresponding to C–C, C–O, and O–C=O bonds, respectively. Combined with the organic oxygen observed in the O 1s spectrum, it can be concluded that propylene glycol is adsorbed on the sample surface. Figures 5 and 6 show that the main composition of the passivation film on the surface of 304 stainless steel remains largely consistent under different pH conditions,

 doi:10.20944/preprints202606.0260.v1

consisting primarily of Fe and Cr oxides and hydroxides; however, the relative content of each component changes with pH. At pH = 4.8, the $Cr(OH)_3/Cr_2O_3$ ratio is the lowest, which may be due to the faster dehydroxylation reaction in acidic solutions [35]; Furthermore, when the propylene glycol coolant has a pH of 4.8, the Fe^{2+}/Fe^{3+} ratio is highest. This is likely because, at lower pH values, the dissolution rate of Fe^{3+} is faster, and Fe in the inner substrate is oxidized to lower-valent oxides [36].

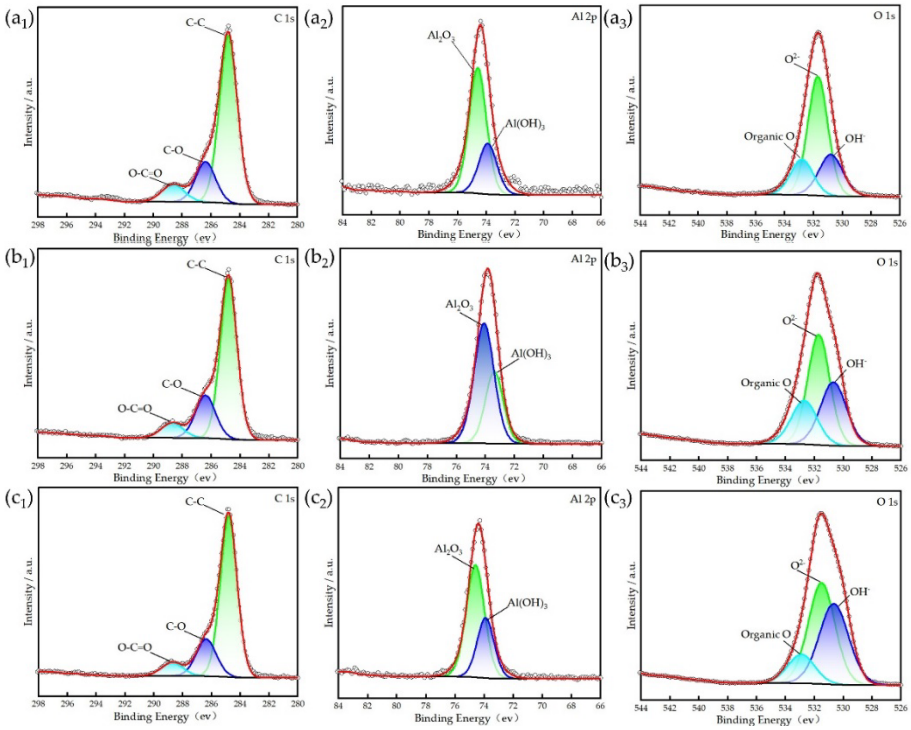

Figure 4. XPS spectra of 6061 aluminum alloy after immersion in propylene glycol coolant with different pH values for 14 days: (a) pH 4.8; (b) pH 6.8; (c) pH 8.8.

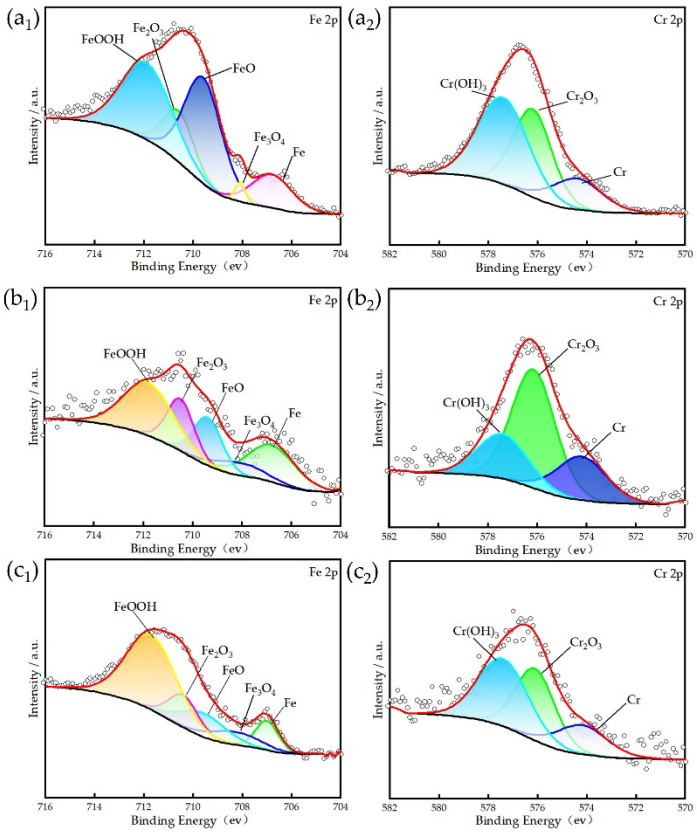

 doi:10.20944/preprints202606.0260.v1

Figure 5. XPS spectra of 304 stainless steel after immersion in propylene glycol coolant with different pH values for 14 days: (a) pH 4.8; (b) pH 6.8; (c) pH 8.8.

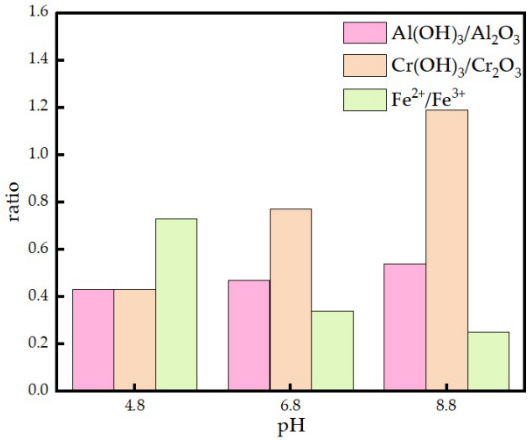

Figure 6. Proportions of different species in XPS spectra under different pH conditions.

3.3. Electrochemical Analysis of Corrosion

Figure 7 and Table 2 show the polarization curves and fitting results for 6061 aluminum alloy and 304 stainless steel in propylene glycol coolant at pH 4.8, pH 6.8, and pH 8.8, respectively. When the pH of the propylene glycol coolant is 4.8, the corrosion potentials of 6061 aluminum alloy and 304 stainless steel are -834 mV and -289 mV, respectively. The significant potential difference between the two materials results in a pronounced galvanic effect, with a corresponding coupled current density of 4933 nA/cm². When the pH of the propylene glycol coolant increased to 6.8, the potential difference between the two materials decreased relatively, and the corresponding coupling current density also decreased to 2581 nA/cm². When the pH of the propylene glycol coolant was increased to 8.8, the corrosion potentials of 6061 aluminum alloy and 304 stainless steel were -717 mV and -217 mV, respectively; the potential difference increased again, leading to an enhanced galvanic corrosion effect. The mixed potential corresponding to the intersection of the polarization curves was -425 mV, and the coupled current density reached 3651 nA/cm².

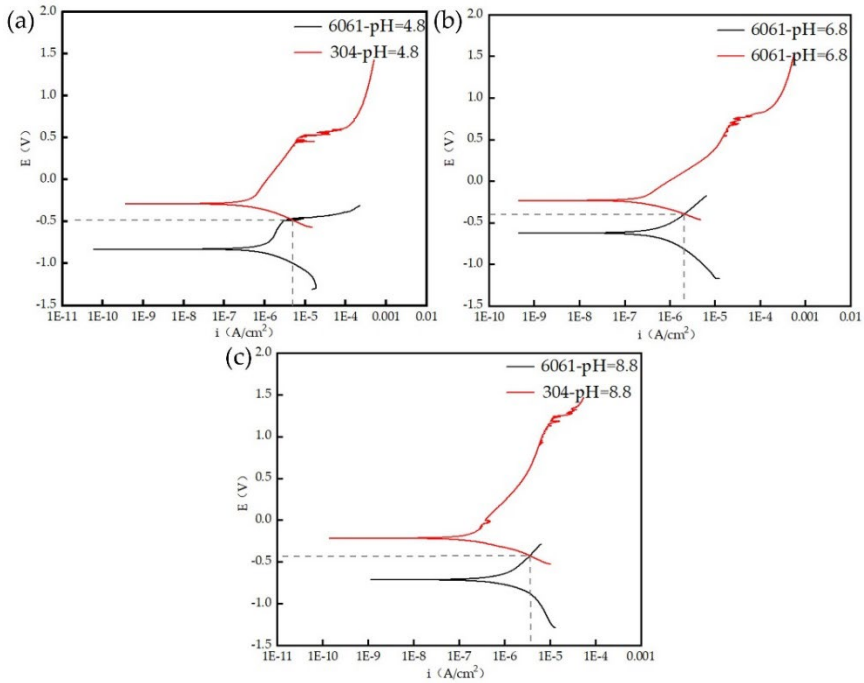

 doi:10.20944/preprints202606.0260.v1

Figure 7. Polarization curves of 6061 aluminum alloy and 304 stainless steel in propylene glycol coolant with different pH values and the changes induced by galvanic corrosion: (a) pH 4.8; (b) pH 6.8; (c) pH 8.8.

Table 2. Fitting results for 6061 aluminum alloy and 304 stainless steel in propylene glycol coolant with different pH values.

Material	pH	Corrosion potential /mV	Mixed potential /mV	Corrosion current density /nA·cm^{-2}	Coupling current /nA·cm^{-2}
6061	4.8	-834	-483	669	4933
	6.8	-625	-397	332	2581
	8.8	-717	-425	483	3651
304	4.8	-289	-483	190	4933
	6.8	-234	-397	132	2581
	8.8	-217	-425	105	3651

Figures 8 and 9, along with Tables 3 and 4, show the polarization curves and fitting results for 6061 aluminum alloy and 304 stainless steel after 20 hours of immersion in propylene glycol coolant at different pH levels, under both coupled and uncoupled conditions. The corrosion current density of 6061 aluminum alloy increased after coupling under different pH conditions, indicating that the galvanic effect between the two materials significantly accelerated the corrosion of 6061 aluminum alloy after coupling. This galvanic effect was most pronounced under acidic conditions and weakest under near-neutral conditions. Furthermore, the corrosion current density of 304 stainless steel after coupling remained consistently low, indicating that 304 stainless steel acts as a cathode in the galvanic system, thereby inhibiting corrosion and maintaining a stable passivated state.

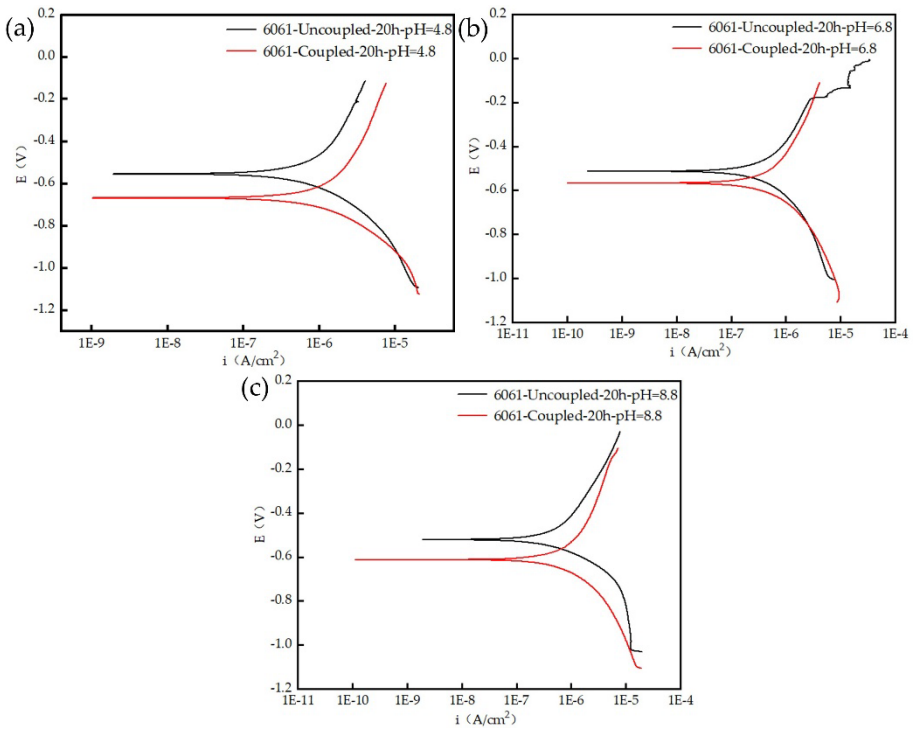

Figure 8. Polarization curves of 6061 aluminum alloy after immersion in propylene glycol coolant with different pH values for 20 h under coupled and uncoupled conditions.

 doi:10.20944/preprints202606.0260.v1

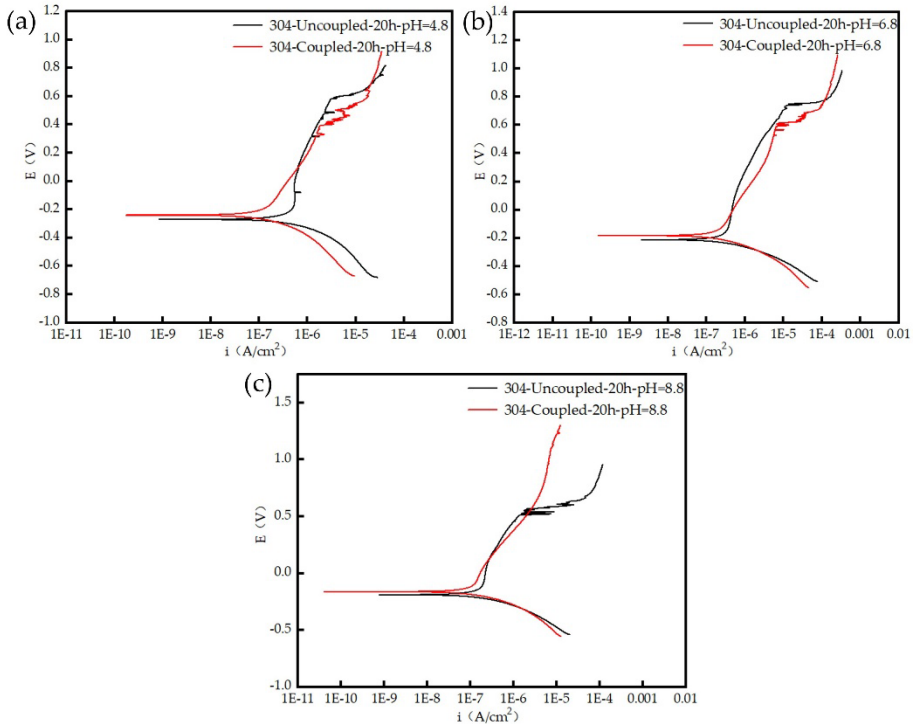

Figure 9. Polarization curves of 304 stainless steel after immersion in propylene glycol coolant with different pH values for 20 h under coupled and uncoupled conditions.

Table 3. Fitting results of polarization curves for 6061 aluminum alloy after immersion in propylene glycol coolant with different pH values for 20 h under coupled and uncoupled conditions.

Test condition	pH	Corrosion potential /mV	Corrosion current density /nA·cm^{-2}
Uncoupled	4.8	-554	431
	6.8	-515	246
	8.8	-520	319
Coupled	4.8	-670	656
	6.8	-570	296
	8.8	-612	394

Table 4. Fitting results of polarization curves for 304 stainless steel after immersion in propylene glycol coolant with different pH values for 20 h under coupled and uncoupled conditions.

Test condition	pH	Corrosion potential /mV	Corrosion current density /nA·cm^{-2}
Uncoupled	4.8	-280	174
	6.8	-214	130
	8.8	-200	102
Coupled	4.8	-245	106
	6.8	-185	103
	8.8	-165	80

Figure 10 shows a schematic diagram of the electrochemical impedance of 6061 aluminum alloy after 20 hours of immersion in propylene glycol coolant at different pH levels, under both coupled and uncoupled conditions. The electrochemical impedance of the 6061 aluminum alloy was fitted using the equivalent circuit shown in Figure 11, and the fitting results are shown in Figure 12. Here, R_s represents the resistance of the propylene glycol coolant, R_f represents the resistance of the oxide film on the 6061 aluminum alloy, and R_{ct} represents the charge transfer resistance at the surface of

 doi:10.20944/preprints202606.0260.v1

the 6061 aluminum alloy matrix. Due to the presence of a certain "diffusion effect," the constant-phase element Q_{f1} represents the interfacial capacitance of the metal-oxide film, and the constant-phase element Q_{f2} represents the interfacial capacitance at the surface of the metal matrix. Furthermore, the commonly used polarization resistance R_p represents the resistance of the system during electrochemical reactions, and polarization resistance $R_p = R_f + R_{ct}$. The smaller the value of R_p, the higher the degree of corrosion in the system and the greater the corrosion rate. As shown in Figures 10 and 12, in propylene glycol coolants with different pH values, both the oxide film resistance Rf and the polarization resistance R_p of 6061 aluminum alloy in the coupled state are smaller than those in the uncoupled state. This indicates that 6061 aluminum alloy consistently acts as the anode in the three types of propylene glycol coolants with pH = 4.8, pH = 6.8, and pH = 8.8 propylene glycol coolants, with electrons flowing from the 6061 aluminum alloy to the 304 stainless steel, resulting in increased corrosion of the 6061 aluminum alloy. Furthermore, when the propylene glycol coolant pH is 4.8, the polarization resistance (R_p) of the 6061 aluminum alloy in the coupled state decreases by approximately 65% compared to that in the uncoupled state; when the propylene glycol coolant pH is 6.8, the difference in polarization resistance (R_p) between the two states of the 6061 aluminum alloy is less than 50%. This may be due to the fact that the aluminum passivation film is easily dissolved by H^+ and Cl^- in an acidic environment, leading to a significant decrease in the stability of the oxide film.

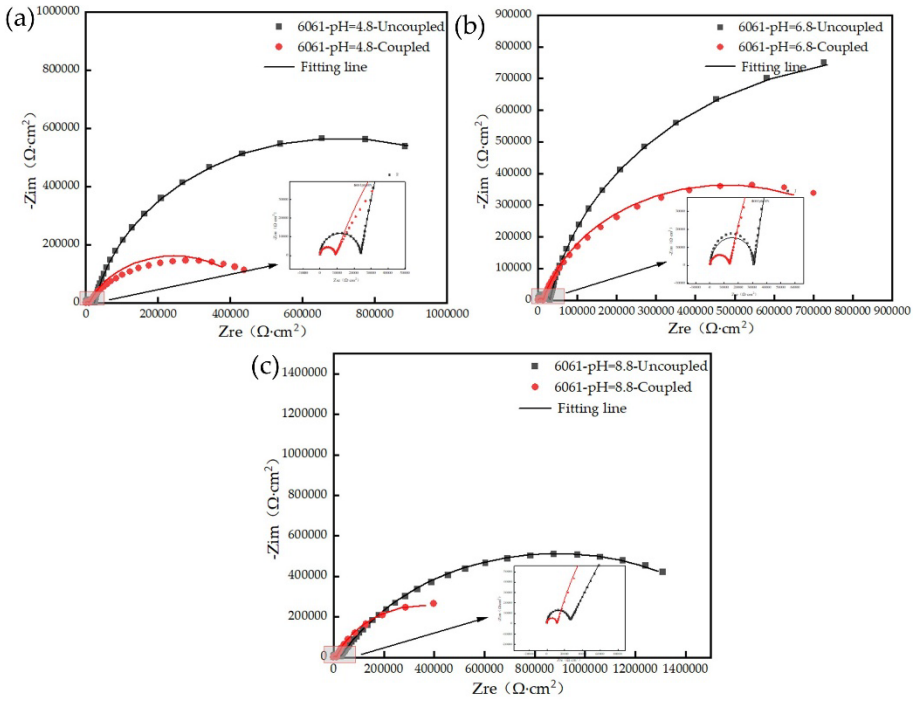

Figure 10. Electrochemical impedance spectra of 6061 aluminum alloy after immersion in propylene glycol coolant with different pH values for 20 h under uncoupled and galvanically coupled conditions: (a) pH 4.8; (b) pH 6.8; (c) pH 8.8.

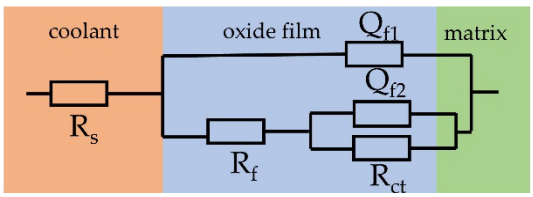

Figure 11. Equivalent circuit models for 6061 aluminum alloy in propylene glycol coolant.

 doi:10.20944/preprints202606.0260.v1

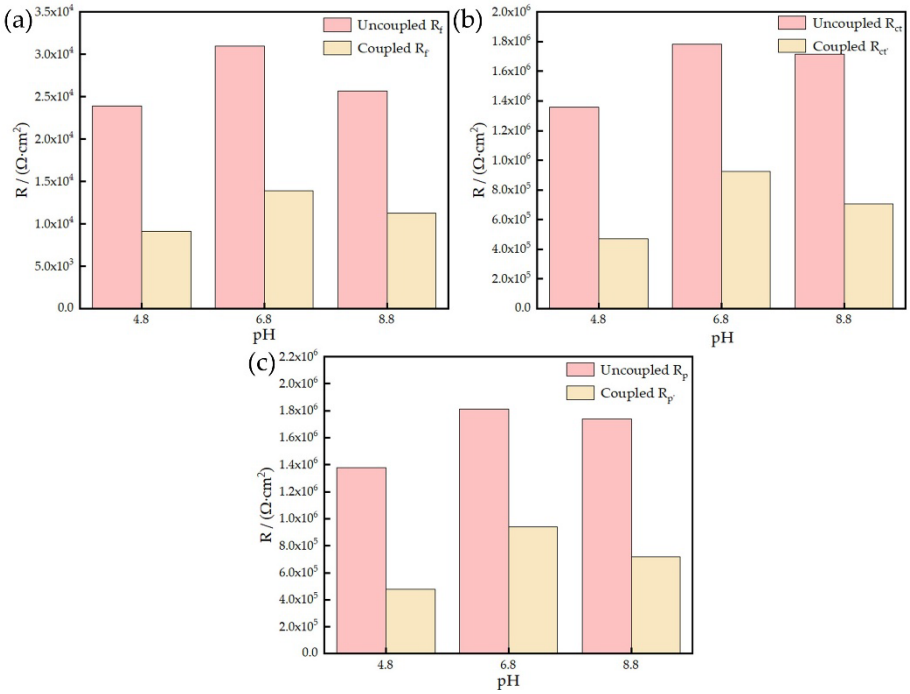

Figure 12. EIS fitting results of 6061 aluminum alloy after immersion in propylene glycol coolant with different pH values for 20 h under uncoupled and galvanically coupled conditions: (a) oxide film resistance, R_f; (b) charge transfer resistance, R_{ct}; (c) polarization resistance, R_p.

Figure 13 shows a schematic diagram of the electrochemical impedance of 304 stainless steel after 20 hours of immersion in propylene glycol coolant at different pH levels, under both coupled and uncoupled conditions. The electrochemical impedance of 304 stainless steel was fitted using the equivalent circuit shown in Figure 14, and the fitting results are shown in Figure 15. Figures 13 and 15 demonstrate that the electrochemical impedance of 304 stainless steel varies under different pH conditions. In the uncoupled state, as the pH increased from 4.8 to 6.8, the polarization resistance R_p of 304 stainless steel increased; when the pH further increased to 8.8, the polarization resistance R_p increased further, indicating that the passivation film on the surface of 304 stainless steel is more stable under near-neutral and weakly alkaline conditions; R_p was minimal under acidic conditions, indicating that 304 stainless steel has a stronger tendency to corrode at pH = 4.8. Under the same pH conditions, both the oxidation film resistance (R_f) and the charge transfer resistance (R_{ct}) of 304 stainless steel in the coupled state were greater than those in the uncoupled state. This indicates that when 304 stainless steel forms a galvanic couple with 6061 aluminum alloy, it primarily acts as the cathode, and its anodic dissolution process is suppressed, resulting in a milder degree of surface corrosion.

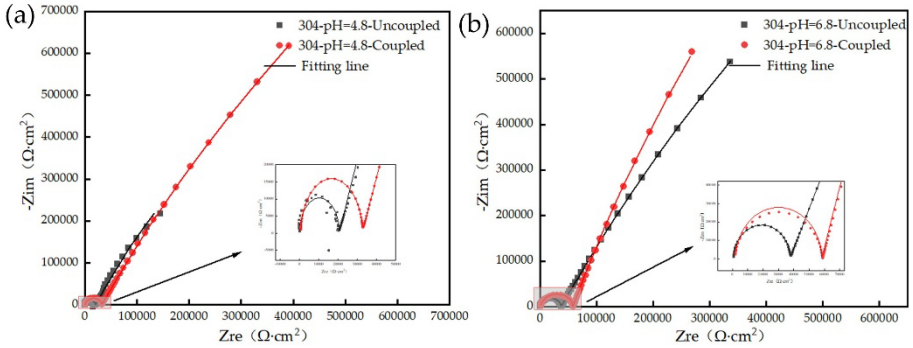

 doi:10.20944/preprints202606.0260.v1

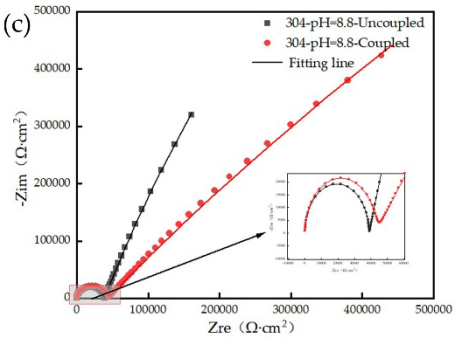

Figure 13. Electrochemical impedance spectra of 304 stainless steel after immersion in propylene glycol coolant with different pH values for 20 h under uncoupled and galvanically coupled conditions: (a) pH 4.8; (b) pH 6.8; (c) pH 8.8.

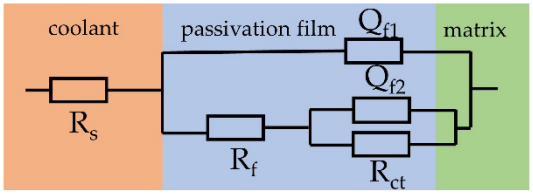

Figure 14. Equivalent circuit models for 304 stainless steel in propylene glycol coolant.

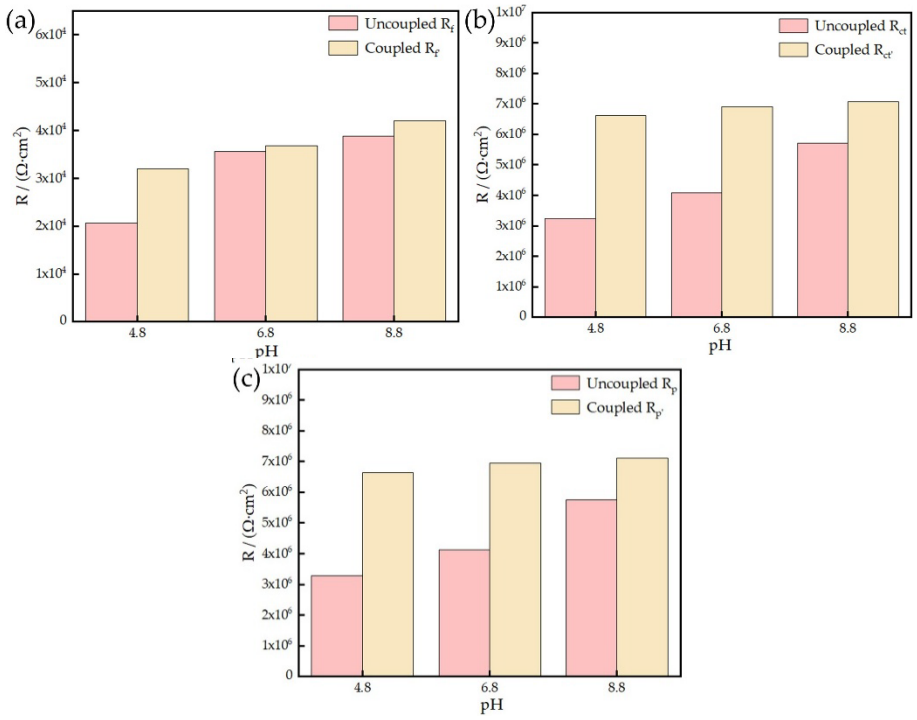

Figure 15. EIS fitting results of 304 stainless steel after immersion in propylene glycol coolant with different pH values for 20 h under uncoupled and galvanically coupled conditions: (a) oxide film resistance, R_f; (b) charge transfer resistance, R_{ct}; (c) polarization resistance, R_p.

3.4. Evaluation of Galvanic Corrosion Sensitivity

Figure 16 shows a schematic diagram of the thermocouple current and potential for a 6061 aluminum alloy/304 stainless steel thermocouple pair in propylene glycol coolant at pH values of 4.8, 6.8, and 8.8. At the beginning of the test, the galvanic current of the 6061 aluminum alloy/304 stainless steel couple in propylene glycol coolants with three different pH values fluctuated to some extent, all showing a trend of first increasing and then decreasing; as the test duration increased, the galvanic

 doi:10.20944/preprints202606.0260.v1

current of the couple in the propylene glycol coolant tended to stabilize. This is because, when the specimens first came into contact with the coolant, the oxide film on the surface of the 6061 aluminum alloy and the passivation film on the surface of the 304 stainless steel had not yet reached a stable state, and the processes of anodic dissolution and cathodic reduction were relatively active. As the immersion time increased, a relatively stable oxide film gradually formed on the surface of the 6061, and the passivation film on the surface of the 304 also tended to stabilize, with the system gradually reaching a dynamic equilibrium. Using Equation (1) to calculate the galvanic current density of the galvanic couple in propylene glycol coolants with pH values of 4.8, 6.8, and 8.8, the results were 3.49 μA/cm², 2.03 μA/cm², and 2.14 μA/cm², respectively. Referring to Table 1 to assess their galvanic corrosion sensitivity, the corrosion sensitivity of the galvanic couple in propylene glycol coolants at pH 6.8 and pH 8.8 is classified as Grade C, while in the propylene glycol coolant at pH 4.8, the corrosion sensitivity increases to Grade D. The test results indicate that propylene glycol coolant with a pH of 4.8 exhibits the highest corrosivity toward the 6061 aluminum alloy/304 stainless steel galvanic couple; however, the change in pH did not alter the anode and cathode roles of the couple, meaning that 6061 aluminum alloy consistently acts as the anode material and 304 stainless steel consistently acts as the cathode material in propylene glycol coolant.

As shown in Figure 16b, the galvanic potential of the galvanic couple in propylene glycol coolant at pH 6.8 and pH 8.8 eventually stabilized at -0.29 V and -0.34 V, respectively; the difference in galvanic potential between the two pH conditions was not significant; The galvanic potential of the pair in propylene glycol coolant at pH 4.8 eventually stabilized near -0.42 V. That is, the galvanic potential of the 6061 aluminum alloy and 304 stainless steel pair was lowest in propylene glycol coolant at pH 4.8, indicating the greatest tendency for galvanic corrosion between the two, which is consistent with the results of the galvanic current test.

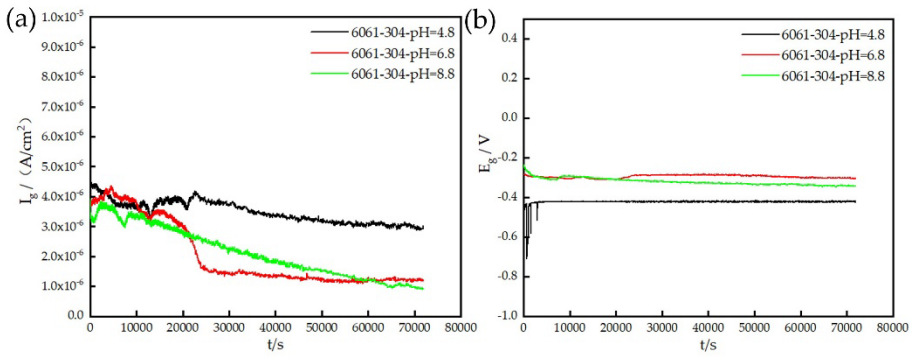

Figure 16. Galvanic current and galvanic potential of the 6061 aluminum alloy/304 stainless steel galvanic couple in propylene glycol coolant with different pH values: (a) galvanic current; (b) galvanic potential.

4. Discussion

In an acidic propylene glycol coolant with a pH of 4.8, the oxide film on the surface of 6061 aluminum alloy undergoes acid dissolution first, as shown by the following reaction:

$$Al_2O_3 + 6H^+ \rightarrow 2Al^{3+} + 3H_2O \quad (2)$$

$$Al(OH)_3 + 3H^+ \rightarrow Al^{3+} + 3H_2O \quad (3)$$

Once the protective film on the specimen's surface is damaged, the exposed aluminum substrate undergoes anodic dissolution, while the cathode continues to reduce dissolved oxygen. The reaction is as follows:

$$Al \rightarrow Al^{3+} + 3e^- \quad (4)$$

 doi:10.20944/preprints202606.0260.v1

$$O_2 + 2H_2O + 4e^- \rightarrow 4OH^- \quad (5)$$

Under pH 4.8 conditions, H+ continuously erodes the surface protective film, causing the aluminum matrix to dissolve continuously and exacerbating corrosion. When the specimen is coupled with 304 stainless steel, electrochemical test results show that the potential of 6061 aluminum alloy is more negative under acidic conditions; it continues to act as an anode, dissolving to form Al^{3+}, while 304 stainless steel consistently acts as a cathode, undergoing an oxygen reduction reaction. Under acidic conditions, the surface film of the 6061 aluminum alloy is severely damaged by H^+, resulting in the most pronounced anodic activation. Meanwhile, although the 304 stainless steel acts as a cathode and does not dissolve, an oxygen reduction reaction continuously occurs on its surface, consuming electrons and driving the 6061 aluminum alloy to continuously lose electrons. Consequently, both the rate of electron generation at the anode and the rate of electron consumption at the cathode are high within the system, leading to the maximum galvanic current and exacerbating the degree of corrosion.

For a weakly alkaline propylene glycol coolant with a pH of 8.8, the oxide film on the surface of 6061 aluminum alloy is no longer damaged by acidity; however, since aluminum is an amphoteric metal, the $Al(OH)_3$ and Al_2O_3 on its surface undergo an alkaline dissolution reaction, which can be expressed as:

$$Al(OH)_3 + OH^- \rightarrow \left[Al(OH)_4\right]^- \quad (6)$$

$$Al_2O_3 + 2OH^- + 3H_2O \rightarrow 2\left[Al(OH)_4\right]^- \quad (7)$$

When the surface protective film dissolves, the aluminum substrate dissolves to form Al^{3+}, and the cathode continues to undergo an oxygen reduction reaction to produce OH^-. The OH^- generated by the cathodic reaction then combines with Al^{3+} to form a new corrosion product film. However, this film is unstable and continues to be broken down by the solution. Consequently, the surface film of 6061 aluminum alloy is constantly forming and breaking down, reducing its protective effect and increasing the degree of corrosion compared to near-neutral conditions. When coupled with 304 stainless steel, the 6061 aluminum alloy continues to dissolve as the anode, while the 304 stainless steel still undergoes the oxygen reduction reaction. Compared to pH = 6.8, under pH = 8.8 conditions, the surface film of the 6061 aluminum alloy undergoes alkaline dissolution due to the action of OH^-, and the anode activity is re-enhanced; At the same time, the passivation film on the surface of 304 stainless steel becomes more stable, allowing its cathodic oxygen-reduction reaction to proceed more continuously. Consequently, the galvanic current in the system increases again compared to pH 6.8, and galvanic corrosion intensifies.

5. Conclusions

This study investigates the corrosion behavior of 6061 aluminum alloy, 304 stainless steel, and their galvanic couples in propylene glycol coolants at pH 4.8, pH 6.8, and pH 8.8. The conclusions are as follows:

(1) Under different pH conditions, compared to uncoupled 6061 aluminum alloy, the coupled 6061 aluminum alloy exhibited increased corrosion weight loss, corrosion pit depth, and corrosion current density, while polarization resistance decreased; that is, the 6061 aluminum alloy consistently acted as the anode and underwent accelerated corrosion; The corrosion severity of 304 stainless steel under both coupled and uncoupled conditions was relatively mild, significantly less than that of 6061 aluminum alloy.

(2) XPS results indicate that as the pH of the propylene glycol coolant increases, the corrosion products of the 6061 aluminum alloy remain unchanged, consisting of $Al(OH)_3$ and Al_2O_3; for 304 stainless steel, the main components of the passivation film remain unchanged under different pH conditions.

 doi:10.20944/preprints202606.0260.v1

(3) As the pH of the propylene glycol coolant increases, the galvanic current between 6061 aluminum alloy and 304 stainless steel in the coolant first decreases and then increases, while the galvanic potential first increases and then decreases. Furthermore, 6061 aluminum alloy consistently acts as the anode and 304 stainless steel as the cathode in the galvanic couple, with no reversal of the anode and cathode occurring. For propylene glycol coolants with pH values of 4.8, pH = 6.8, and pH = 8.8, the corresponding galvanic corrosion sensitivity grades are Grade D, Grade C, and Grade C, respectively.

CRediT authorship contribution statement

Hao Miao: Writing—review & editing. Cong Shao: Investigation & Validation. Hao Yu: Validation. Wang Qian He: Validation. Zheng Qiao Jin: Investigation & Project administration. Kui Xiao: Project administration & Review.

Declaration of Competing Interest

The authors declare that they have no known competing financial interests or personal relationships that could have appeared to influence the work reported in this paper.

Acknowledgements

Research on Compatibility of Liquid Cooled Working Fluid Supported by ZTE Research Fund.

References

1. Bashkirtseva, N.; Sladovskaya, O.; Ovchinnikova, Y.; Vazetdinova, L.; Yusupov, S. Corrosion inhibitors for water–glycol based cooling systems. Chem. Technol. Fuels Oils 2017, 52, 751–755. https://doi.org/10.1007/s10553-017-0769-7.
2. Shia, D.; Yang, J.; Sivapalan, S.; Soeung, R.; Amoah-Kusi, C. On cold plate corrosion with propylene glycol/water coolant. In Proceedings of the 2021 20th IEEE Intersociety Conference on Thermal and Thermomechanical Phenomena in Electronic Systems (iTherm), 2021; pp. 212–219. https://doi.org/10.1109/itherm51669.2021.9503231.
3. Shia, D.; Yang, J.; Sivapalan, S.; Soeung, R.; Amoah-Kusi, C. Corrosion study on single-phase liquid cooling cold plates with inhibited propylene glycol/water coolant for data centers. J. Manuf. Sci. Eng. 2021, 143, 111012. https://doi.org/10.1115/1.4051059.
4. Zhou, R.; Chen, Y.; Zhang, J.; et al. Research progress in liquid cooling technologies to enhance the thermal management of LIBs. Mater. Adv. 2023, 4, 4011–4040. https://doi.org/10.1039/D3MA00299C.
5. Srinivasan, R.; Kollo, T. Predicting galvanic corrosion of aluminum using accelerated laboratory electrochemical experiments. ECS Meet. Abstr. 2023, MA2023-01, 1485. https://doi.org/10.1149/ma2023-01181485mtgabs.
6. Zuo, H.; Fan, J.; Liu, F.; Gong, M.; Zheng, X.; Meng, J.; Yang, G.; Liu, X. Corrosion behavior of 3A21 aluminum alloy in water–ethylene glycol coolant under simulated engine working conditions. Int. J. Electrochem. Sci. 2021, 16, 21062. https://doi.org/10.20964/2021.06.05.
7. Zhang, G.A.; Xu, L.Y.; Cheng, Y.F. Investigation of erosion–corrosion of 3003 aluminum alloy in ethylene glycol–water solution by impingement jet system. Corros. Sci. 2009, 51, 283–290. https://doi.org/10.1016/j.corsci.2008.10.026.
8. Liu, Y.; Cheng, Y.F. Effects of coolant chemistry on corrosion of 3003 aluminum alloy in automotive cooling system. Mater. Corros. 2010, 61, 574–579. https://doi.org/10.1002/maco.200905323.
9. Liu, Y.; Cheng, Y.F. Characterization of passivity and pitting corrosion of 3003 aluminum alloy in ethylene glycol–water solutions. J. Appl. Electrochem. 2011, 41, 151–159. https://doi.org/10.1007/s10800-010-0215-6.
10. Gong, A.; Zhou, M.; Wu, Q.; Wang, G. Study on the corrosion behavior of stainless steel in coolant. Proc. SPIE 2024, 13420, 1342008. https://doi.org/10.1117/12.3055019.
11. Monticelli, C.; Brunoro, G.; Frignani, A.; Zucchi, F. Corrosion behaviour of the aluminium alloy AA 6351 in glycol/water solutions degraded at elevated temperature. Mater. Corros. 1988, 39, 379–384. https://doi.org/10.1002/maco.1980390805.
12. Khomami, M.N.; Danaee, I.; Attar, A.A.; Peykari, M. Kinetic and thermodynamic studies of AISI 4130 steel alloy corrosion in ethylene glycol–water mixture in presence of inhibitors. Met. Mater. Int. 2013, 19, 453–464. https://doi.org/10.1007/s12540-013-3011-0.

 doi:10.20944/preprints202606.0260.v1

13. Fowles, J.R.; Banton, M.I.; Pottenger, L.H. A toxicological review of the propylene glycols. Crit. Rev. Toxicol. 2013, 43, 363–390. https://doi.org/10.3109/10408444.2013.792328.
14. Khutko, M.; Gordiienko, O.; Sydoruk, T.; Ransky, A. Cooling liquids with improved ecological and operating properties. Visnyk Vinnytsia Polytech. Inst. 2021, 156, 32–40. https://doi.org/10.31649/1997-9266-2021-156-3-32-40.
15. Shahi, P.; Heydari, A.; Hinge, C.; Chinthaparthy, L.; Modi, H.; Miyamura, H.; Tradat, M.; Chowdhury, U.; Radmard, V.; Agonafer, D.; Rodriguez, J. Thermal, hydraulic and reliability analysis of single-phase liquid coolants for direct-to-chip cold plate cooling in high-performance computing systems. In Proceedings of the ASME 2023 International Technical Conference and Exhibition on Packaging and Integration of Electronic and Photonic Microsystems, 2023. https://doi.org/10.1115/ipack2023-110576.
16. He, F.; Wu, N.; Zhou, Z.; Wang, J. Experimental investigation on transpiration cooling using propylene glycol aqueous solution. Int. J. Therm. Sci. 2021, 164, 106890. https://doi.org/10.1016/j.ijthermalsci.2021.106890.
17. Shahroom, A.F.; Rahman, N.A.; Mansor, M.; Rahman, M.S.A. Modelling analysis of propylene glycol as a cooling media for battery thermal management system in electric vehicles. Arab. J. Sci. Eng. 2024, 50, 10541–10553. https://doi.org/10.1007/s13369-024-09703-1.
18. Gündem, A.; Hoşöz, M.; Keklik, E. Performance comparison of propylene glycol–water and ethylene glycol–water mixtures as engine coolants in a flat-tube automobile radiator. Int. J. Automot. Sci. Technol. 2021, 5, 147–156. https://doi.org/10.30939/ijastech.914901.
19. Zhang, G.A.; Xu, L.Y.; Cheng, Y.F. Mechanistic aspects of electrochemical corrosion of aluminum alloy in ethylene glycol–water solution. Electrochim. Acta 2008, 53, 8245–8252. https://doi.org/10.1016/j.electacta.2008.06.043.
20. Tian, Y.; Li, H.; Wang, S.; Fan, Y. Erosion–corrosion behavior of aluminum in a 50 °C ethylene glycol aqueous solution simulating cooling water in HVDC transmission. Mater. Corros. 2021, 72, 1899–1907. https://doi.org/10.1002/maco.202112453.
21. Zaid, B.; Saidi, D.; Benzaid, A.; Hadji, S. Effects of pH and chloride concentration on pitting corrosion of AA6061 aluminum alloy. Corros. Sci. 2008, 50, 1841–1847. https://doi.org/10.1016/j.corsci.2008.03.006.
22. Rong, H.; Fan, W.; Shan, B.; Yang, J.; Ding, R.; Zhao, X. Galvanic corrosion behavior and numerical simulation of 5083 aluminum alloy and Q235 steel in 3.5% NaCl solution. Mater. Corros. 2023, 74, 766–776. https://doi.org/10.1002/maco.202213438.
23. Li, Y.; Teng, J.; Wang, J.; Wang, H.; Liu, Q.; Lai, R.; Yang, B.; Wang, Z.; Li, Y. Interfacial corrosion behavior of aluminum/steel joints prepared by solid-state additive manufacturing. Corros. Sci. 2025, 244, 112650. https://doi.org/10.1016/j.corsci.2024.112650.
24. Stajuda, L.; Levchenko, D.; Kubiak, P.; Siczek, K.; Bogusławski, G.; Kuchar, M.; Woźniak, M.; Szymczak, M.; Ozuna, G.; Siczek, K. Composition, features, problems, and treatment related to cooling fluid—a review. Combust. Engines 2023. https://doi.org/10.19206/ce-169185.
25. Ikeuba, A.I. AFM and EIS investigation of the influence of pH on the corrosion film stability of Al4Cu2Mg8Si7 intermetallic particle in aqueous solutions. Appl. Surf. Sci. Adv. 2022, 11, 100291. https://doi.org/10.1016/j.apsadv.2022.100291.
26. Ikeuba, A.I.; Zhang, B.; Wang, J.; Han, E.H.; Ke, W. Electrochemical, TOF-SIMS and XPS studies on the corrosion behavior of Q-phase in NaCl solutions as a function of pH. Appl. Surf. Sci. 2019, 490, 535–545. https://doi.org/10.1016/j.apsusc.2019.06.089.
27. Miao, H.; Yu, H.; Wang, H.; Zheng, J.; Shao, C.; Xiao, K. Corrosion behavior of 7A09 aluminum alloy exposed to propylene glycol coolant at different conditions. Int. J. Electrochem. Sci. 2025, 20, 101105. https://doi.org/10.1016/j.ijoes.2025.101105.
28. Zhang, X.; Liu, X.; Dong, W.; Hu, G.; Yi, P.; Huang, Y.; Xiao, K. Corrosion behaviors of 5A06 aluminum alloy in ethylene glycol. Int. J. Electrochem. Sci. 2018, 13, 10470–10479. https://doi.org/10.20964/2018.11.64.
29. Kolics, A.; Besing, A.S.; Baradlai, P.; Haasch, R.; Wieckowski, A. Effect of pH on thickness and ion content of the oxide film on aluminum in NaCl media. J. Electrochem. Soc. 2001, 148, B251–B259. https://doi.org/10.1149/1.1376118.

 doi:10.20944/preprints202606.0260.v1

30. Ruiz, A.; Ortiz, A.; Genesca, J.; Montoya, R. Numerical study of local pH variations in a galvanic carbon steel–aluminum alloy system under immersion conditions. ECS Trans. 2021, 101, 373–381. https://doi.org/10.1149/10101.0373ecst.
31. Ortiz, A.; Ruiz-Garcia, A.; Genesca, J.; Montoya, R. Acidification of the electrolyte in the carbon steel/aluminum alloys galvanic couple: Modeling and experimental study. In Proceedings of CORROSION 2021, 2021. https://doi.org/10.5006/c2021-16334.
32. Ruiz-Garcia, A.; Esquivel-Peña, V.; Genesca, J.; Montoya, R. Advances in galvanic corrosion of aluminum alloys. Electrochim. Acta 2023, 456, 142227. https://doi.org/10.1016/j.electacta.2023.142227.
33. Shi, L.; Yang, X.; Song, Y.; Liu, D.; Dong, K.; Shan, D.; Han, E. Effect of corrosive media on galvanic corrosion of complicated tri-metallic couples of 2024 Al alloy/Q235 mild steel/304 stainless steel. J. Mater. Sci. Technol. 2019, 35, 1886–1893. https://doi.org/10.1016/j.jmst.2019.04.022.
34. Sakairi, M.; Sasaki, R.; Kaneko, A.; Seki, Y.; Nagasawa, D. Evaluation of metal cation effects on galvanic corrosion behavior of the A5052 aluminum alloy in low chloride ion containing solutions by electrochemical noise impedance. Electrochim. Acta 2014, 131, 123–129. https://doi.org/10.1016/j.electacta.2014.02.010.
35. Yang, W.P. Resistance to pitting and chemical composition of passive films of a Fe–17%Cr alloy in chloride-containing acid solution. J. Electrochem. Soc. 1994, 141, 2669–2676. https://doi.org/10.1149/1.2059166.
36. Wang, Z.; Zhou, Z.Q.; Zhang, L.; Hu, J.Y.; Zhang, Z.R.; Lu, M.X. Effect of pH on the electrochemical behaviour and passive film composition of 316L stainless steel. Acta Metall. Sin. Engl. Lett. 2019, 32, 585–598. https://doi.org/10.1007/s40195-018-0794-5.